Directional Microphone Array for Acoustic Studies of Wind Tunnel Models

Paul T. Soderman* and Stephen C. Noble†
NASA Ames Research Center, Moffett Field, Calif.

An end-fire microphone array that utilizes a digital time delay system has been designed, fabricated, and evaluated for measuring noise in wind tunnels. The directional response of both a four- and eight-element linear array of microphones has enabled substantial rejection of background noise and reverberations in the NASA Ames 40- by 80-ft Wind Tunnel. In addition, it is estimated that four- and eight-element arrays reject 6 and 9 db, respectively, of microphone wind noise, as compared with a conventional omnidirectional microphone with nose cone. Array response to two types of jet engine models in the wind tunnel is presented. Comparisons are made of array response to loudspeakers in the wind tunnel and in freefield.

Introduction

ACOUSTIC studies of aircraft models are becoming an important part of wind tunnel investigations at numerous facilities in this country and abroad.[1,2] Forward speed effects on propulsion noise, and aerodynamically generated noise data are necessary for proper aircraft design. Techniques are evolving for solving various problems associated with wind tunnal noise studies. For example, a major problem with conventional, closed test-section wind tunnels is that drive system noise, microphone wind noise, and source reverberations tend to mask the desired acoustic signals. In some cases, one can predict and account for reverberation levels.[3] Even then, background and wind noise can limit acoustic research in wind tunnels, especially as aircraft engine and airframe noise become lower. This paper describes a measurement technique for discriminating against wind tunnel reverberations and background noise. The technique involves the use of a directional acoustic receiver that has low response to wind noise.

Antenna Design

One way to create a directional receiver is to use an array of microphones that function as an antenna. Microphones, like any antenna sensors, can be arranged geometrically such that proper synthesis of the microphone signals results in a response to sound coming only from a desired region. The use of antennas in closed test sections places two major constraints on the design: 1) the antenna and/or the antenna elements must be aerodynamically shaped for low flow noise and 2) the device should reject unwanted sound from every direction but that of the aircraft model, since background noise and reverberations can strike the array from any angle. These constraints rule out such designs as solid, disk-shaped antennas and systems which have strong back lobes (like broadside arrays). Consequently, we chose to evaluate linear, end-fire arrays of microphones.

A simple but effective linear array of microphones is shown in Fig. 1. This array provides a directional response to sound if the microphone signals are individually time delayed and then summed to give a single output. Time delay for each of n microphones is normally chosen such that sound waves traveling along the array axis sum in phase. Microphone signal delays of 0, t, $2t$, . . . , $(n-1)t$ sec (for microphones 1, 2, 3, . . . , n, respectively, where the nth microphone is the one closest to the sound source) depend only on the speed of sound and microphone spacing, not frequency. Sound waves arriving off axis sum out of phase, and therefore tend to cancel, since the distances between microphones along a ray do not correspond with the time delays chosen for on-axis sound. Hence, the main response is along the array axis ($\alpha=0°$) making the antenna an end-fire array. The device is effective for both random or sinusoidal sound. The response of an end-fire array to a single tone can be written:

$$p(t)=kA\sum_{i=1}^{n}\sin\left[\omega(t+a_i)\right] \tag{1}$$

or, as shown by Kraus[4]:

$$p(t)=kA\frac{\sin(n\psi/2)}{\sin(\psi/2)}\sin\left[\omega t+\frac{\psi(n-1)}{2}\right] \tag{2}$$

where $p(t)$ = array response (pressure or voltage), A = amplitude of sound wave, k = gain of electronic control module, chosen as 1/8 for the eight-element array, n = number of microphones, $\omega=2\pi f$, frequency, $a_i=\tau(1-\cos\alpha)$, $\tau=(i-1)$

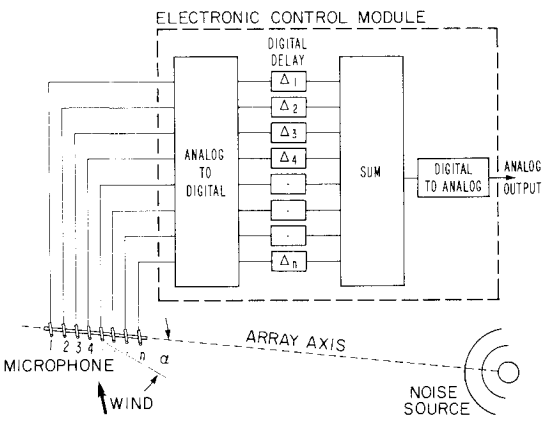

Fig. 1 End-fire microphone array.

Presented as Paper 74-640 at the AIAA 8th Aerodynamic Testing Conference, Bethesda, Maryland, July 8 - 10, 1974; submitted July 17, 1974; revision received October 29, 1974. We are indebted to A. Atencio and M. Falarski of Ames for J-85-5 jet noise data and the turbofan data, respectively. Measurements of the test section response to an acoustic impulse (Fig. 11) were made by D. Bies and R. Sawley of Bolt, Beranek and Newman, Inc. We wish to thank S. Karel of Ames for the computation of the rms value of $p(t)$ in Eq. (5).
Index category: Aircraft Testing, Aircraft Noise, Power Plant.

*Research Scientist, U.S. Army Air Mobility R&D Laboratory.
†Air Force Research Associate, Captain, U.S. Air Force, now at Air Force Avionics Laboratory, Wright-Patterson Air Force Base, Ohio.

d/c, time delay for the ith microphone (ordinary end fire), α = angle between sound ray and array axis (see Fig. 1), d = spacing between microphones, λ = acoustic wave length, c = speed of sound, and $\psi = (2\pi d/\lambda)(1 - \cos\alpha)$.

Antenna theory is well developed.[4] It is known, for example, that the more sensor elements there are in the antenna, the sharper will be the directional response. The longer the array, the better will be the low frequency response. An important parameter affecting directivity is d/λ, the ratio of element spacing to signal wavelength.

Preliminary investigations of a four-element array developed at Ames and reported in Ref. 5 led us to construct and evaluate an eight-element array with improved directional characteristics. Both arrays were investigated in an anechoic chamber and in the Ames 40- by 80-foot Wind Tunnel.

Instrumentation and Apparatus

Each array was comprised of omnidirectional microphones (B&K model 4133) with nose cones mounted to a 2.54 cm (1 in) diam pipe as shown in Fig. 2. The microphone signals were input to the electronic control module, which continually digitized, delayed, summed, and reconverted the resulting signal into analog form. The analog output was an unfiltered,‡ real-time fluctuating voltage that was similar to the microphone signals except for the reduced off-axis sound, as previously discussed. The data were then analyzed in third-octave bands. Delay of each channel from 0 to 10 msec in 0.01 msec steps could be chosen by the operator. Integrated circuit components were used extensively in the control module.

Anechoic Chamber Calibration

Figures 3a-3d show ordinary directional response of the four- and eight-element end-fire arrays measured in the anechoic chamber. "Ordinary" directional response refers to the array with delay settings τ of $(i-1)d/c$, which corresponds to wave propagation time between elements. The measurements were made by rotating the arrays, one at a time, 4.9 m (16 ft) from a fixed loudspeaker. The anechoic chamber had dimensions 5.5 m (18 ft) by 7.6 m (25 ft) by 3.4 m (11 ft) high, wedge tip to wedge tip. The low frequency cut off of the chamber was 150 Hz. At 0°, the arrays were aimed at the source. Figures 3a-3d show that the eight-element array had the better directivity. As predicted by theory, the primary parameter affecting directivity was the ratio of mircophone spacing to wavelength, d/λ. It was shown in Ref. 5 that the same directivity at two different frequencies was maintained if spacing was adjusted to keep d/λ constant. The best directivity occurred for d/λ between 0.22 and 0.88 for the four-element array and d/λ between 0.22 and 3.50 for the eight-element array. Above these limits, side lobes grew (high frequency), and below these limits, the main lobe broadened (low frequency). At $d/\lambda = 0.5$ the front and back lobes were equal and at $d/\lambda = 0.25$ the back lobe was eliminated. These results indicate that microphone spacing should be adjusted for a given acoustic frequency if optimum directivity is desired. Furthermore, previous studies[5] showed that broadband noise must be analyzed in third-octave bands or narrower to achieve optimum d/λ. However, the following wind-tunnel studies showed that the microphone arrays were very effective over a large frequency range even with nonoptimum spacing.

According to Hansen and Woodyard (Ref. 4, p. 81), directivity of an end-fire array can be substantially improved by using an increased time delay of:

$$(i-1)(2\pi d/\lambda + \pi/n)/2\pi f =$$
$$(i-1)(d/c + 1/16f), \text{ for } n = 8 \qquad (3)$$

‡ High-frequency digital noise outside the audio range was filtered out by using a three-pole low-pass filter with a cutoff frequency of 10 kHz.

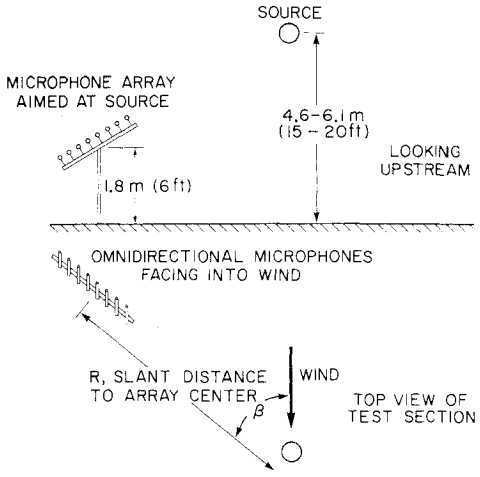

Fig. 2 Typical array location in the Ames 40- by 80- ft Wind Tunnel test section. β is the angle between array axis and wind.

Figure 4 shows that this delay did reduce the width of the main lobe at the expense of minor lobe growth. Since the increased delay is frequency dependent, we decided to use the ordinary delay of Eq. (1), which does not depend on frequency, for the following wind-tunnel studies. One could, conceivably, build a system which automatically adjusts increased delay as a narrow-band filter scans the acoustic signal, but that was beyond the scope of this study.

Wind-Tunnel Measurements

The degree of rejection of unwanted sound in the Ames 40- by 80-ft Wind Tunnel by the arrays was determined by measuring the noise of: 1) a 12-sided loudspeaker system (dodecahedron) mounted near the test section center, 2) GE J85-5 jet engine mounted under an aircraft model wing (Fig. 5), and 3) P&W JT15-D-1 turbo-fan engine (Fig. 6). Details of the engines are presented in Table 1. The individual, omnidirectional microphones with nose cones were aimed into the wind to minimize wind noise as shown in Fig. 2. Figure 2 also defines the slant distance, R, and the array-wind angle, β.

Loudspeaker Source

The electronic gain of the array was adjusted so that at all frequencies the array response along the array axis ($\alpha = 0°$) was equal to that of an omnidirectional microphone with both devices in anechoic space. Measurements were made with the eight-element array aimed at the dodecahedron noise source in the wind tunnel. The lower noise levels measured by the array were caused by partial rejection of source reverberation, microphone wind noise, and wind-tunnel drive noise. Figure 7 shows the array response for 30.5 cm (1 ft) spacing compared to the response of a single microphone. This spacing results in optimum directivity between 500 and 1000 Hz. The dodecahedron free-field output was measured in the anechoic chamber. The data indicate that the array was measuring approximately free-field levels below 3.15 kHz in the wind tunnel at 5.8 m. Above 3.15 kHz, the array measured much less noise that the source generated; this anomalous result was probably caused by an experimental error discussed in a later section. An array with 5.1 cm (2 in) spacing of elements, which would have a suitable narrow main lobe between 3000 and 6000 Hz, had slightly better high-frequency response. However, the 30.5 cm (1ft) spacing gave the better performance overall.

J85-5 Jet Noise

Figure 8a shows the noise generated by the J85-5 jet engine exhausting through a 104-tube noise suppressor nozzle described in Ref. 6. An eight-element array with 30.5 cm (1 ft)

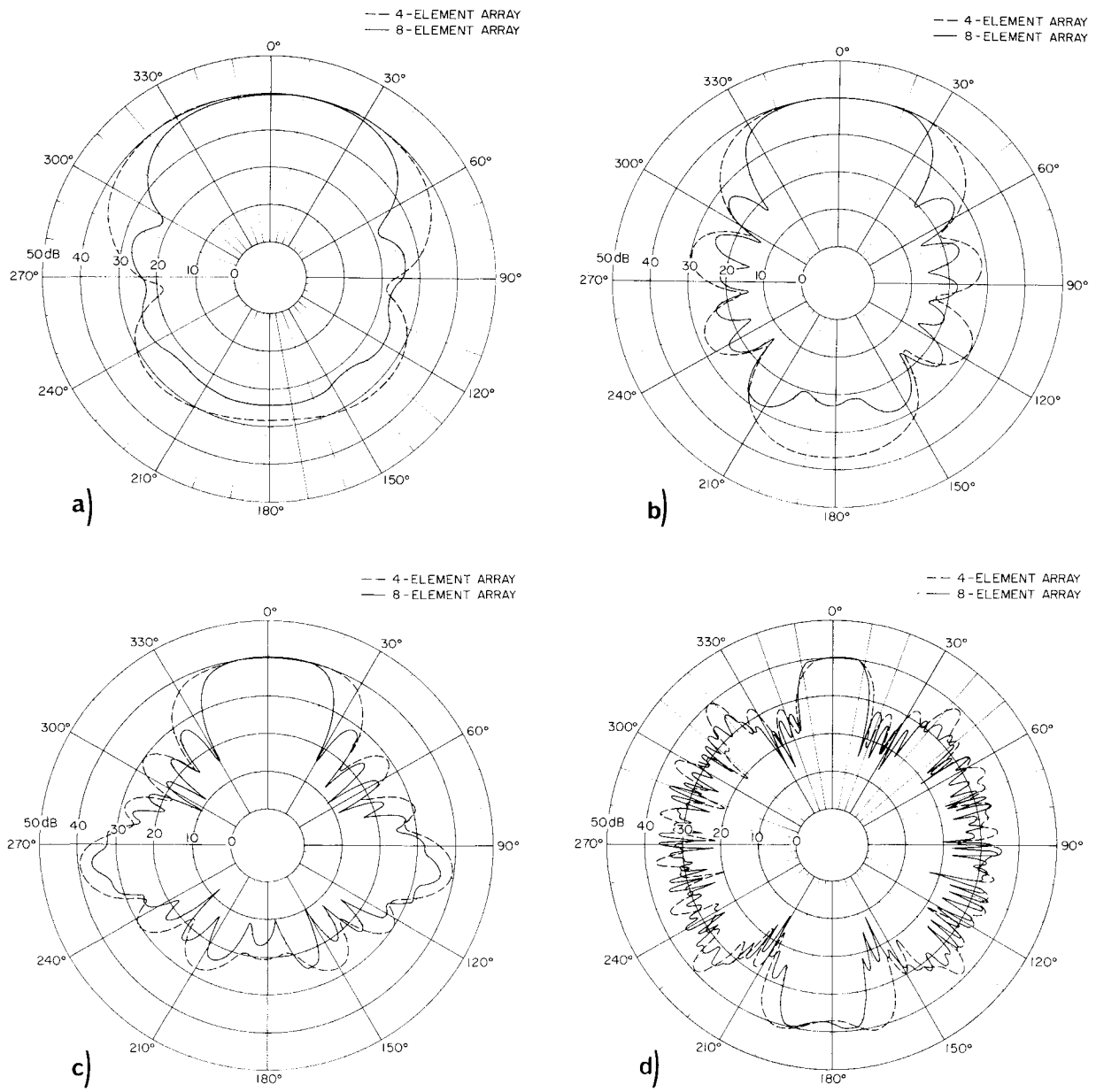

Fig. 3 Sound pressure level directivity pattern of four-and eight- element arrays with 30.5 cm (1 ft) microphone spacing measured in the anechoic chamber. Directivity angle is relative to array axis. Acoustic tone source. a) $f = 250$ Hz, $d/\lambda = 0.22$; b) $f = 500$ Hz, $d)/\lambda = 0.45$; c)$f =$ 1000 Hz, $d/\lambda = 0.89$; d) $f = 4000$ Hz, $d/\lambda = 3.57$.

Table 1 Engine parameters

GE J85-5 Jet		P&W JT15-D-1 Turbo-fan	
Pressure ratio	1.82	Bypass ratio	3
Thrust	9937 N (2234 lb)	Fan diameter	53 cm(21 in)
Jet velocity	527 m/s fs) (1728 fs)	Thrust	3558 N (800 lb)
Compressor rpm	15,636	Fan rpm	10,300

microphone spacing located 9 m (30 ft) from the nozzle (151° relative to the inlet) measured up to 8 db less noise than did an omnidirectional microphone at the same location. The background noise measured by both devices was much below the jet noise levels. With forward speed of 51 m/sec (167 fps) (Fig. 8b), the same array rejected 3 to 10 db of unwanted sound. The data show that the array had a much lower noise floor than did the single microphone because of partial rejection of flow noise and wind-tunnel drive noise. This would allow measurement of quieter sources in the wind tunnel. The rejection of noise by the array occurred over a large frequency range despite the growth of side lobes in the directivity pattern at large values of d/λ. Thus, a fixed microphone spacing can be used to simplify the experimental procedure.

JT 15-D-1 Turbo fan noise

Figure 9 shows the noise generated by the turbofan engine. The measurement was made 7 m (23 ft) from the model and 45° relative to the inlet axis. The eight-element array had 5.1 cm (2 in) microphone spacing for optimum discrimination at higher frequencies. This resulted in poor performance at low frequencies.

Wind Noise

It was not possible during the wind tunnel investigation to separate wind noise rejection from rejection of background and reverberation noise. However, the array should respond

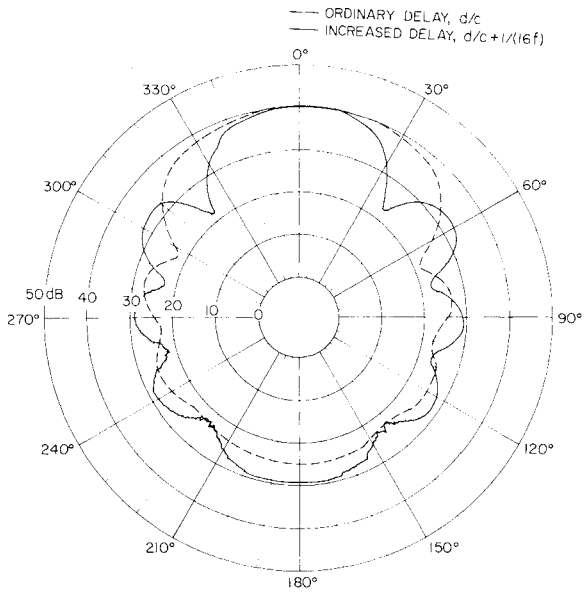

Fig. 4 Effect of increased delay on directivity of eight-element array; $d = 30.5$ cm (1 ft), f = 250 Hz.

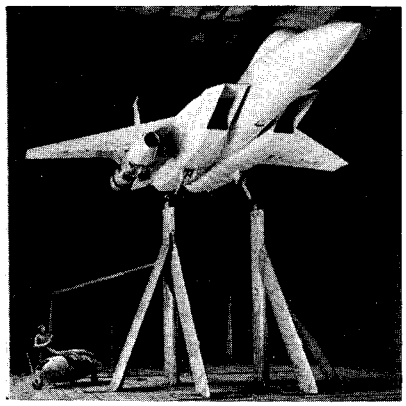

Fig. 5 GE-J85-5 jet engine mounted to aircraft model in the test section.

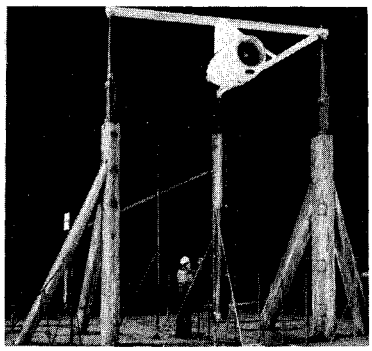

Fig. 6 P&W JT15-D-1 turbofan mounted in test section.

better to sound generated external to the array than to locally generated wind noise because on-axis sound waves add coherently (6 db per doubling of microphone number) while microphone wind noise adds incoherently (3 db per doubling of microphone number). Figure 10 shows the predicted relative response of end-fire arrays to on-axis sound and wind noise.

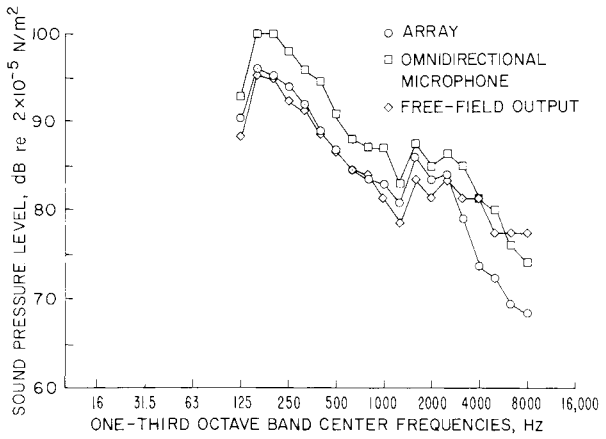

Fig. 7 Response of eight-element array and single microphone to dodecahedron generating octave bands of random (pink) noise in the wind tunnel, $U = 0$, $d = 30.5$ cm, $\beta = 90°$, $R = 5.8$ m (19 ft).

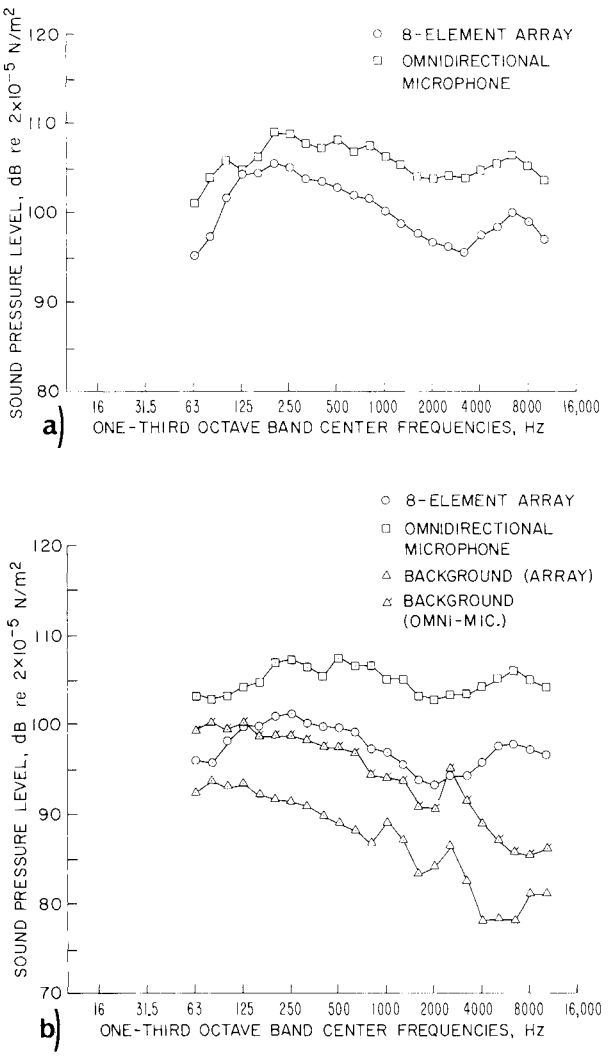

Fig. 8 J85-5 jet noise in the wind tunnel, $d = 30.5$ cm (1 ft), $\beta = 151°$, $R = 9$ m (30 ft); a) $U = 0$; b) $U = 51$ m/sec (167 fps).

Reverberation Rejection

The 40- by 80-ft Wind Tunnel test section is semi-reverberant since most of the reflected noise comes from the steel walls, floor, and ceiling of the test section; a lesser amount of energy returns from the upstream corner. Because

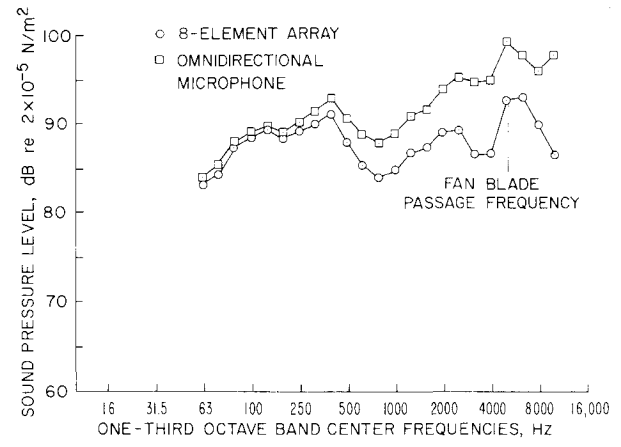

Fig. 9 JT 15-D-1 turbofan noise in the wind tunnel, $d = 5.1$ cm (2 in), $\beta = 45,^\circ$ $R = 7$m (23 ft).

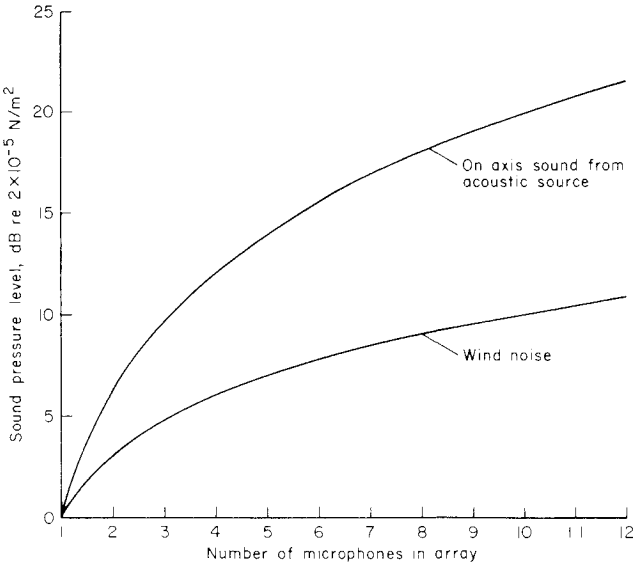

Fig. 10 Predicted array output in excess of single microphone output.

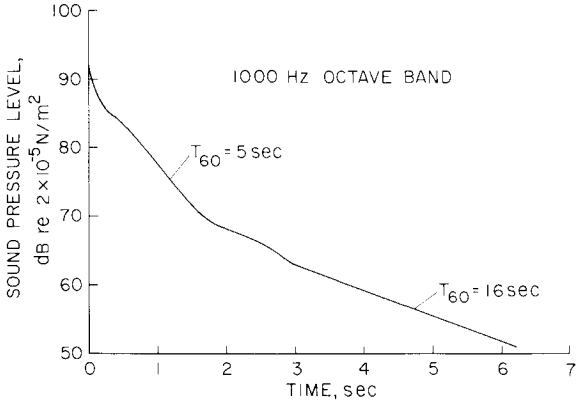

Fig. 11 Reverberation decay in wind tunnel test section. Omnidirectional microphone used.

of the size and geometry of the facility, the reverberant field is fairly diffuse. No acoustic material was installed in the wind tunnel. Figure 11 shows the test section response to an acoustic impulse (balloon pop) at 1000 Hz. The initial acoustic decay rate was controlled by reflections in the test section. The second decay rate was controlled by reflections from the upstream corner. For a steady-state source, the reverberant field was up to 5db above the direct field at 5.8 m (19 ft) as shown in Fig. 7.

An analytical method was devised in Ref. 5 for predicting the response of an end-fire array in an ideal reverberant field so that discrimination against a reverberant field could be estimated. Since antenna transmission is analogous to reception (principle of reciprocity), it can be assumed for calculation purposes that the array generates sound. The sound emitted by a source in anechoic space is equivalent in terms of amplitude and directivity to the sound received in a reverberant space. Imagine the emitted sound pressure levels integrated over a sphere surrounding a directional array (i.e., the sound power) in anechoic space compared to the sound power of an omnidirectional source adjusted to give the same pressure level as the array along the array axis ($\alpha = 0°$). Obviously, the omnidirectional source would emit the greater sound power by some amount Δdb. Due to the principle of reciprocity, it follows that this increment of sound power is equal to the difference in sound pressure levels measured by an omnidirectional microphone and a directional array in a reverberant space, both adjusted to have equal sensitivity at $\alpha = 0°$. Thus, the emitted sound power levels of the array and an omnidirectional source were calculated in the following manner.

The array directivity pattern measured in the anechoic chamber was used to represent transmission directivity. Sound power was calculated using the following relationship:[7]

$$LW = \overline{Lps} + 20 \log R + 11 \tag{4}$$

where

LW = total sound power level, db *re* 10^{-12} watt

R = radius of sound measurement locations on a sphere surrounding the source, meters

$\overline{Lps}$ = average mean-square sound pressure level over the sphere, db re 2×10^{-5} N/m^2.

Each sound pressure measurement was associated with the proper portion of the sphere surface area. It was assumed that the sound pressure levels on a circle around the array were typical of the levels on a sphere around the array with the array generating sound. The calculated sound power level was then substracted from the sound level of an omnidirectional source which generates the same noise level as the array at $\alpha = 0°$ (i.e., on the array axis).

Figure 12 shows that the calculated results agree fairly well with the measured values of noise rejection using the four-element array (data from Ref. 5). The differences between calculated and measured data were probably due to the wind-tunnel test section being semi-reverberant rather than reverberant as assumed for the calculations. The estimated discrimination of approximately 10 db by the eight-element array could not be verified experimentally, since the rever-

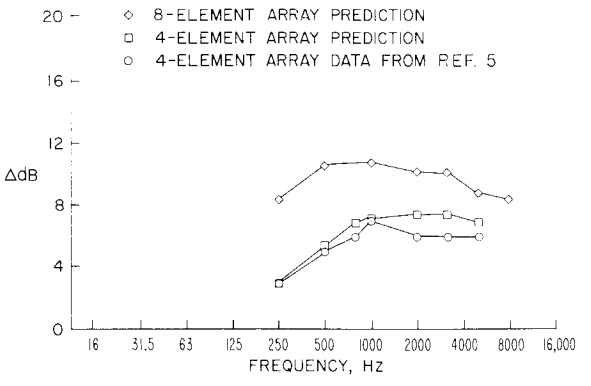

Fig. 12 Calculated and measured noise rejection of arrays in a reverberant field; $\Delta db = db_{omnidir\ mic} - db_{array}$.

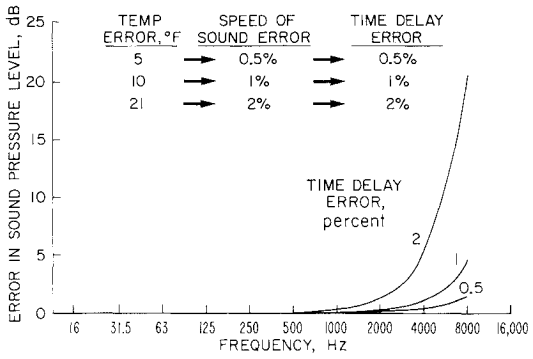

Fig. 13 Decrease in on-axis sound level due to error in time delay for eight-element array with 30.5 cm (1 ft) microphone spacing. Time delay is affected by temperature, wind, and microphone spacing.

berant field was only about 5 db above the direct sound field in these investigations (see Fig. 7).

Error Analysis

The preceding analysis assumes that the signal time delays equal the wave propagation time between appropriate microphones. In practice, wave propagation time estimates can be in error if the temperature and wind velocity are not properly incorporated in the choice of time delay. Time delay can also be in error if the microphone spacing is not exact. All this can degrade both the on-axis response and the directivity pattern. Consider Eq. (1) in another form:

$$p(t)=kA\sum_{i=1}^{n}\sin\left[\omega(t+b_i)\right] \tag{5}$$

where $b_i=D_i\cos\alpha/C_1-(i-1)D/C$; D_i = actual distance between ith and first microphone ($i=1$); D = assumed spacing between microphones; C = assumed speed of sound; C_1 = actual speed of sound, $C_o-U\cos\beta$ (plane waves), $[C_o^2-U^2\sin^2\beta]^{1/2}-U\cos\beta$ (spherical waves); C_o = speed of sound in still air, const. $(T)^{1/2}$; β = angle between wind vector and array axis; T = absolute temperature; and U = wind speed. If the proper wind and temperature are incorporated in the assumed sound speed then $C_1=C$. The error due to misalignment of the array (incorrect α) was found to be negligible.

A computer program was devised to calculate the root-mean-square value of $p(t)$ in Eq. (5) and the resulting pressure level. Figure 13 shows the calculated decrease in sound pressure level at $\alpha=0°$ for various amounts of error in time delay $[(i-1)D/C]$.[§] Since a 1% error in time delay would be caused by a 10°F error in temperature or a 3 to 5 m/sec (10 to 16 fps) error in wind speed, accuracy of the array at high frequencies requires careful experimental technique. Also, the phase characteristics of the microphones must be similar at all frequencies.

In retrospect, Figs. 13 and 7 indicate that the high-frequency data of Ref. 5 may be in error. The reported good noise rejection of the four-element array above 5 kHz may have been the result of incorrect time delay due to speed-of-sound estimates which decreased the received signal.

Conclusions

A digital delay system for end-fire acoustic reception, in which arrays of conventional microphones were used, rejected substantial amounts of background noise, reverberations, and wind noise in the Ames 40- by 80-ft Wind Tunnel. The array performance depended on the ratio of microphone spacing to wavelength and array orientation in the wind tunnel. An eight-element array with 30.5 cm (1 ft) microphone spacing rejected 3 to 10 db of unwanted sound from 63 Hz to 10 kHz. However, the data above 3.15 kHz were inconclusive since the array performance at high frequencies was quite sensitive to speed of sound estimates, which may have been in error by 1 to 2%. The best directivity was attained by using a time delay dependent on acoustic frequency. However, good results over a wide frequency range were achieved with a time delay that is dependent only on microphone spacing and the speed of sound. It was estimated that, using the latter time delay, an eight-element array should reject 9 db of microphone wind noise and up to 11 db of reverberations.

References

[1] Bender, J. and Arndt, R. E. A., "Aeroacoustic Research in Wind Tunnels: A Status Report." CR 114575, Feb. 1973, NASA.

[2] Falarski, M. D., Koenig, D. G., and Soderman, P. T., "Aspects of Investigating STOL Noise Using Large-Scale Wind-Tunnel Models," TM X-62,164, June 1972, NASA.

[3] Atencio, A., Jr. and Soderman, P. T., "Comparison of Aircraft Noise Measured in Flight Test and in the NASA Ames 40- by 80-Foot Wind Tunnel," AIAA Paper 73-1047, Seattle, Wash., 1973.

[4] Kraus, J. D., *Antennas,* McGraw-Hill, New York, 1950.

[5] Soderman, P. T. and Noble, S. C., "A Four-Element End-Fire Microphone Array for Acoustic Measurements in Wind Tunnels," TM X-62, 331, Jan. 1974, NASA.

[6] Wilcox, F. A., "Comparison of Ground and Flight Test Results Using a Modified F106B Aircraft," AIAA Paper 73-1305, Las Vegas, Nev., 1973.

[7] *Noise and Vibration Control,* edited by L. L. Beranek, McGraw-Hill, New York, 1971.

[§] Equation (3) can be substituted for D/C in Eq. (5) to compute effect of increased time delay.